13th World Conference on Earthquake Engineering
Vancouver, B.C., Canada
August 1-6, 2004
Paper No. 3093

SEISMIC RETROFIT OF MASONRY INFILL WALLS USING ADVANCED COMPOSITES

WAEL W. EL-DAKHAKHNI[1], AHMAD A. HAMID[2] AND MOHAMED ELGAALY[3]

SUMMARY

Masonry infill panels in frame structures have been long known to affect strength, stiffness and ductility of the infilled frame structures. In seismic areas, ignoring the composite action is not always on the safe side, since the interaction between the panel and the frame under lateral loads dramatically changes the dynamic characteristics of the composite structure and hence its response to seismic loads. It has been generally recognized that infill walls enhance the response of frame buildings in low to moderate seismic regions, yet they exhibit poor seismic performance under high seismic demand because of the degradation of stiffness, strength and energy dissipation capacity observed under cyclic loading. Their degradation results from the progressive damage of the masonry wall and the deterioration of the panel-frame interfaces. This paper presents a retrofitting methodology of concrete masonry infill panels using fiber reinforced polymer (FRP) laminates. The method is expected to enhance the system behaviour under strong earthquake loads as has been shown by test results. This method also prevents the undesirable failure modes and facilitates modeling by eliminating the anisotropic nature of masonry panels and clearly defining the behaviour of the retrofitted system.

Keywords: Composites; GFRP laminates, Infill walls; Masonry; Steel frames; Seismic hazard; Seismic retrofit.

INTRODUCTION

Masonry infill panels can be found as interior and exterior walls in reinforced concrete and steel framed structures. Since they are normally considered as architectural elements, their presence is often ignored by structural engineers. However, they normally interact with the surrounding frame when the structure is subjected to earthquake loads; the resulting system is referred to as an infilled frame.

[1] Post-doctoral Fellow, McMaster University Centre for Effective Design of Structures, Hamilton, Ontario, Canada, L8S 4L7. E-mail: eldak@mcmaster.ca
[2] Professor and Associate director of McMaster University Centre for Effective Design of Structures, On leave, Department of Civil and Architectural Engineering, Drexel University, Philadelphia, PA. E-mail: hamida@ mcmaster.ca
[3] Professor, Department of Civil and Architectural Engineering, Drexel University, Philadelphia, PA, 19104, USA. E-mail: elgaalym@drexel.edu

This study presents a proposed design methodology of retrofitting **C**oncrete **M**asonry-**I**nfilled **S**teel **F**rame (CMISF) structures using Fiber-Reinforced Polymer (FRP) laminates in order to enhance their seismic response. The retrofitting technique using FRP laminates aims to create an engineered infill wall with well defined stiffness and ultimate load capacity, by means of strengthening and eliminating the undesirable failure modes.

Based on the knowledge gained from both analytical and experimental studies during the last five decades, different failure modes of the masonry-infill walls can be categorized into two main distinct failure modes, namely:

1. Corner crushing mode (CC mode), represents crushing of the infill in at least one of its loaded corners. This mode is usually associated with infill of weak masonry blocks surrounded by a frame with weak joints and strong members.

2. Sliding shear mode (SS mode), represents horizontal sliding shear failure through bed joints of a masonry infill. This mode is associated with infill of weak mortar joints and frame with strong members and joints.

CONCEPTUAL DESIGN OF RETROFITTED CMISF

The process of investigating possible failure modes with the uncertainty associated with the shear strength of the walls is a tedious but necessary job to determine the governing mode and consequently the governing failure load and the supply, to meet a certain demand. Hence, the FRP retrofitting scheme suggested herein seems like an optimum solution, since, if properly designed, the FRP laminate should reduce the uncertainty in behaviour, and suppress, as much as possible, the brittle behaviour of masonry panels, thus reducing the seismic hazard associated with failure and simplifying the modeling process.

The effect of the proposed retrofitting technique is comprised of four different aspects, namely:

1. Preventing undesirable, brittle failure modes. This is achieved by restricting failure modes to the *CC* mode, with well-defined strength, stiffness and ductility. This, in turn, will result in eliminating the uncertainty associated with the modeling process.
2. Eliminating the anisotropic behaviour of masonry, by essentially eliminating the effects of the shear-compression interaction in the mortar joints. This will transform the anisotropic masonry wall into an orthotropic wall, thus simplifying modelling.

3. Reducing the P-Δ effect as well as the sudden drift resulting from the *SS* modes under lateral loads.

4. Preventing out-of-plane failure or spalling of masonry blocks, which is, by itself, a major source of seismic hazard.

The following subsections address the FRP effect on defining the *CC* mode behaviour after retrofitting and eliminating all other failure modes by proper design of the FRP laminate.

EXPERIMENTAL PROGRAM

The experimental program consisted of two main phases. In the first phase, three different types of assemblages were tested: namely; prisms loaded normal and parallel to the bed joints, and direct shear

specimens. The test specimens were chosen to represent typical loading cases of masonry walls in the two orthogonal directions as well as shear loading along the weak mortar bed joints as shown in Fig. 1. A total of 57 full-scale specimens were constructed in the laboratory and tested to failure under monotonically increasing loads. Out of these specimens, 24 were loaded normal to the bed joints (shown in Fig. 1-b), 9 were loaded parallel to the bed joints (shown in Fig. 1-c), and 24 were loaded under direct shear (shown in Fig. 1-d). Standard C-90 hollow concrete masonry blocks and Type S mortar were used in the construction of the assemblages.

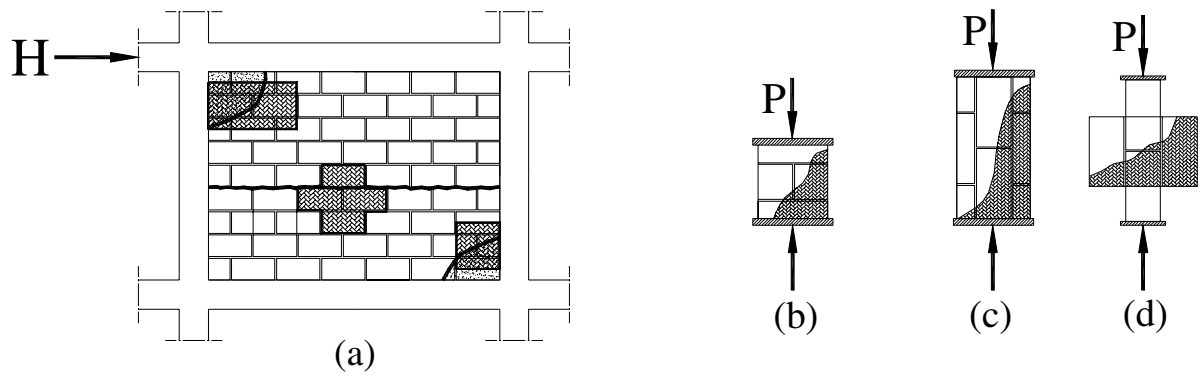

Fig. 1: Test specimens: a) Inside an infill wall; b) Loading normal to bed joint; c) Loading parallel to bed joint; d) Loading in shear; and e) Shear specimen construction

The second phase of the experimental program deals with testing of full-scale concrete masonry infilled steel frames. Six 3.6 x 3.0 m (12 ft x 10 ft) single story single bay frames were tested under cyclic lateral load. No shear connection was provided between the retrofitted wall and the frames and the FRP was cut to the exact dimensions of the wall without adhering the laminate to the steel members.

Before applying the FRP, the specimens surface were first cleaned from dust and mortar protrusions manually using a wire brush. In this preparation, attention was focused on cleaning the joints and removing excessive mortar and loose particles from the wall surface. A light layer of epoxy resin was then applied to the wall using a hand held paint roller to the wall surfaces. A mixture of the epoxy resin and silica fume was then used to fill the joints and smooth the prepared surface before applying the composite materials. Prior to application on the walls, the dry fabrics were cut to length and the epoxy was worked into it with a paint roller till saturation, this was necessary to ensure good bonding with the wall surface. The first layer of the fabric was applied so that the fibers were perpendicular to the masonry bed joints. This configuration was concluded from the shear test specimens previously investigated.

The behaviour and experimental results of three specimens are presented in the following paragraphs.

Test Setup and Instrumentation

The test setup including loading system and dimensions is shown in Fig. 2. The frame members and connections were designed and constructed according to the specification of the American Institute of Steel Construction (AISC [1]). The frames were designed for gravity load only to represent existing design philosophy in low and sometimes moderate seismic risk regions.

The columns and the beams of the frames were made of (W10x22) shape. The lateral load was applied by means of a servo-controlled hydraulic actuator with a 1500 kN (325 kips) and a stroke of ±200 mm (± 8 in).

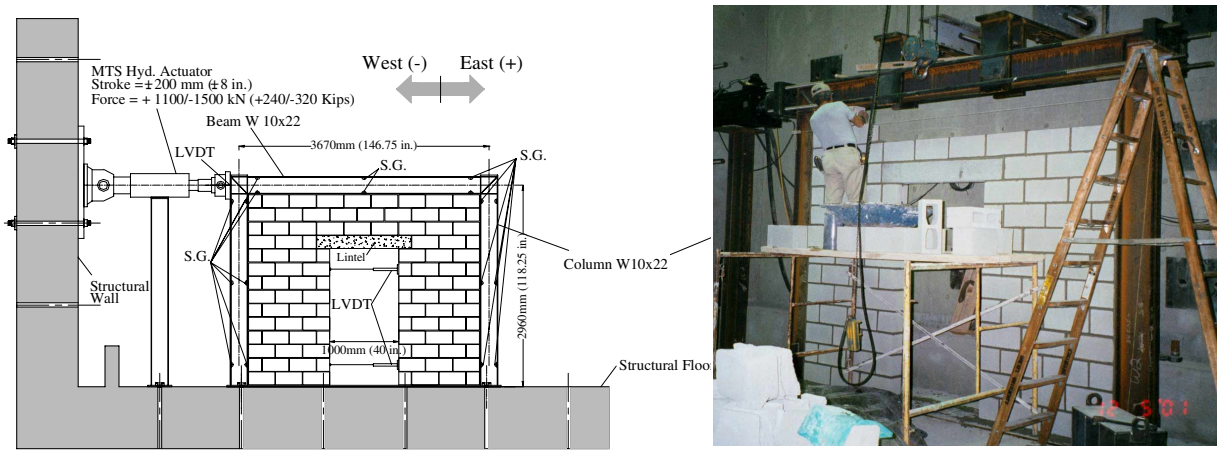

(a) (b)

Fig. 2: Test setup: a) Schematic diagram; and b) Specimen Construction

Displacement Protocols

The sequential phased displacement technique developed by Porter and Tremel [2] was the load history adopted for this study. In this procedure, groups of drift cycles are organized around peak amplitudes that are gradually increased to failure. Peak amplitudes after the initial elastic displacements are tied to the first major event, which can be interpreted as the first instance of significant damage. Two stages of displacement protocol were designed for all specimens. After the first stage of displacements (Fig. 3-a) was applied, the damage level was then investigated for each specimen and based on that it was decided weather or not to continue with the second stage (Fig. 3-b).

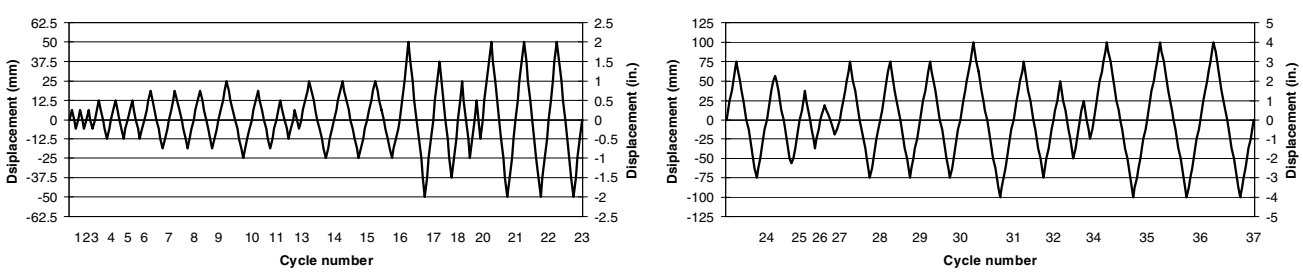

(a) **(b)**

Fig. 3: Sequential phased displacement protocols: a) First stage; and b) Second stage

TEST RESULTS

Phase 1

While many fiber configurations were used, the Tyfo® SEH-51A with the Tyfo® S epoxy matrix, resulted in the most desirable behaviour, since they resulted in:

1. Effectively increasing the shear strength of shear assemblages up to 14 folds (see Fig 4-a). The shear failure was eliminated and compression failure in the top and bottom blocks of the shear specimen occurred.

2. Improving the compression strength of the face shells by supplying the tensile strength required to stabilize the out-of-plane buckling of the individual face shells, thus preventing the out-of-plane buckling failure. This increased the compressive strength by 75% and 90% for the compression prisms normal and parallel to the bed joint, respectively.

3. Preventing the catastrophic failure of the masonry-FRP composite assemblages in contrast to their URM counterparts. This particular FRP laminate resulted in a gradual prolonged failure under shear, and a stronger wall under compression with apparent post peak strength. The FRP laminates maintain the wall integrity, contain and localize the damage of the URM walls even after ultimate failure (see Fig 4-b).

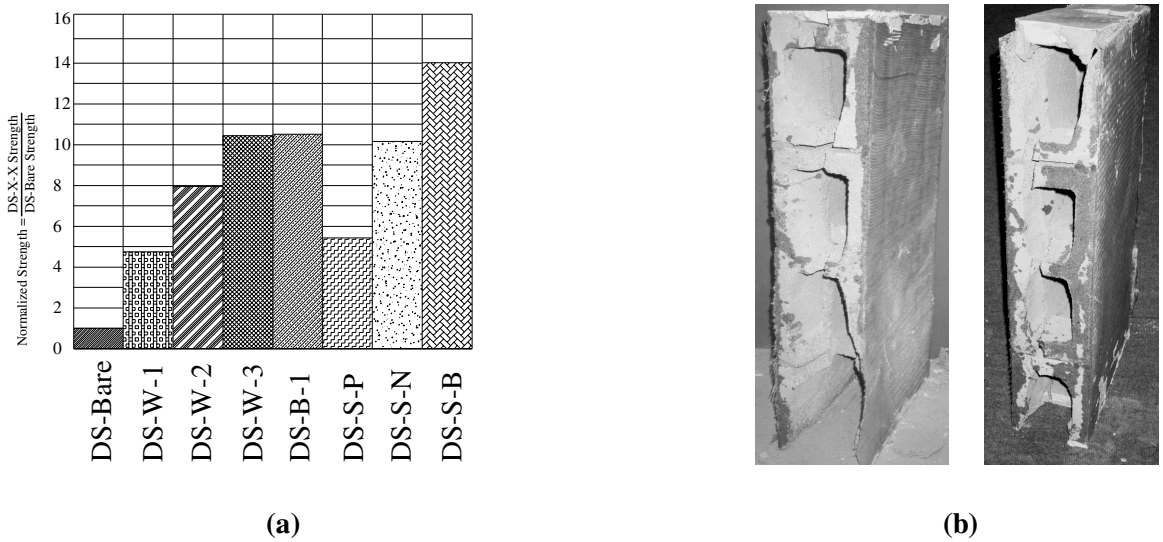

Fig. 4: Effect of the FRP retrofitting on strength of assemblages: a) Shear assemblages; and b) Failure of prisms in compression

Phase 2

The first specimen was the bare steel frame. The first stage of displacement was applied to the frame and no signs of concentrated damage or yielding appeared at any part. The second set of loading was applied and signs of permanent plastic deformations were noticed by the end of the loading stage. The frame was then investigated closer and the column flanges in the vicinity of the beam column connections appeared to suffer permanent local buckling. Furthermore the load-deflection relation showed that the specimen started yielding at 68 mm (2.7 in.) at which plastic hinge developed in the top of the columns.

The second specimen was the frame with solid unretrofitted infill wall. When the first set of displacement was applied to the specimen, signs of failure began at +12.5 mm (+0.5 in.) as a 45° inclined crack initiated at the bottom east corner. At a -12.5 mm (-0.5 in.) the other diagonal crack was formed in the panel starting from the west bottom corner. As the rest of the 12.5 mm (0.5 in.) cycles continued, these diagonal cracks were joined by some horizontal sliding cracks developed along the bed joints in the vicinity of the wall's mid-height. At +18.75 mm (+0.75 in.), a major shear-slip in the bed joint occurred between the

sixth and seventh courses from top as shown in Fig. 5-a. At the 50 mm (2.0 in.) displacement level, marking the end of this stage, severe corner crushing occurred with parts of the wall spalling out of the frame and this appeared to be the ultimate capacity of the specimen. As the rest of the cycles at this displacement level continued, most of the blocks and all mortar joints were severely cracked with many parts missing after face shell spalling and the wall was essentially behaving as a non-connected separate blocks.

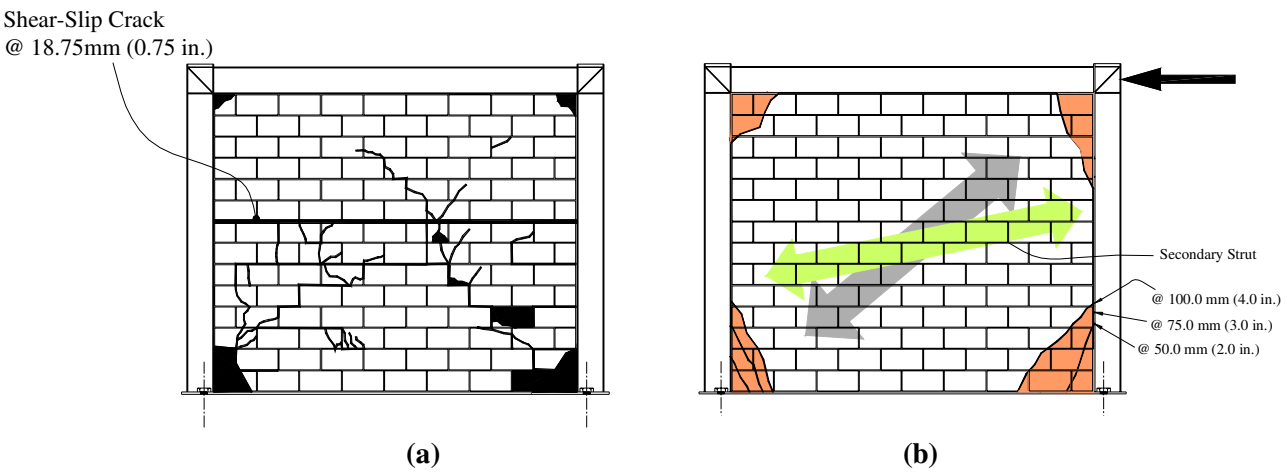

Fig. 5: Infilled frames failure modes: a) The unretrofitted specimen; and b) The retrofitted specimen

The third specimen was the retrofitted specimen in this test program. Because the FRP laminate was applied on both sides no visible signs of failure was observed up to 18.75 mm (0.75 in.) displacement, however, sounds thought to be webs splitting were heard at 12.5 mm (0.5 in.) and 18.75 mm (0.75 in.) displacement levels. While the laminate in the corners remained attached to the face shell at 25 mm (1.0 in) yet the corners appeared to suffer minor out-of-plane walking-out of the frame as the frame pushed against the wall. This behaviour continued to appear throughout the load stage with no signs of failure occurring at the wall except at the corners at 50 mm (2.0 in.) and continuing through the last 100 mm (4.0 in.) cycles as shown in Fig. 5-b.

3-D FE MODELING

A detailed 3-D finite element (FE) analysis of the behaviour of the specimen discussed in this study was conducted by El-Dakhakhni and Drysdale [3] to evaluate the behaviour of infilled frame. The FE model load-deflection behaviour vs. the experimentally obtained one for the bare steel specimen is shown in Fig.6-a. In addition the model accurately predicts the permanent plastic deformation at the column bases (Fig 6-b), the formation of the plastic hinge at the beam column connection (Fig 6-c), and the permanent camber of the base plate (Fig 6-d) similar to the experimental observations. It is worth mentioning that although the behaviour of the steel material was modeled as a bilinear stress-strain relation with initial and secant Young's modulus of 200 GPa and 2 GPa respectively, yet the over all load-deflection relation is not exactly bilinear, however this represent the actual frame behaviour due to the semi-rigid connection at the bottom that resulted from the column bases being neither pinned nor totally fixed. The FE model load-deflection behaviour vs. the experimentally obtained one is shown in Fig.7-a and 7-b for the unretrofitted and the retrofitted specimens, respectively.

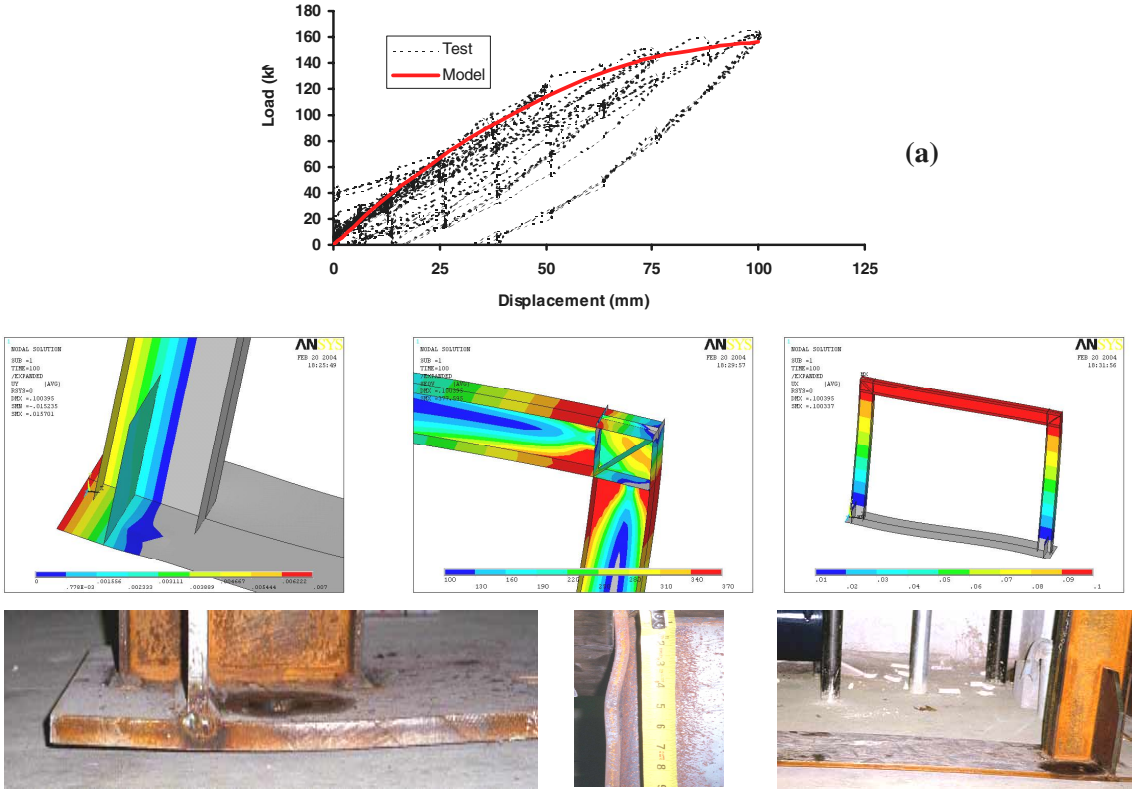

Fig. 6: Experimental vs. FE results for bare frame specimen: a) Load-deflection relation; b) Column base upward displacement; c) Column top yielding; and d) Base plate camber

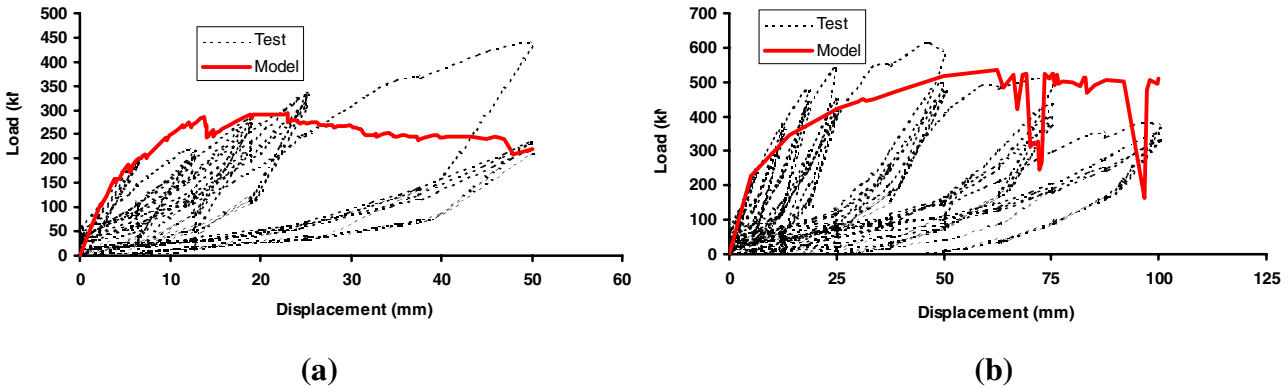

Fig. 7: Experimental vs. FE predicted load-deflection: a) Unretrofitted specimen and b) Retrofitted specimen

EQUIVALENT STRUT MODEL

Because 3-D FE analysis is not practical for multi-storey structures, and because of its practicality and ease of implementation in analysis, the diagonal strut concept will be utilized herein to present a method of analysis of CMISF retrofitted with FRP laminates. In fact under reversed seismic loading, the corner crushing might be accompanied with shear failure of the infill. The presence of the FRP laminate should, however, prevent any shear failure. The increase in stiffness can be investigated by applying the diagonal strut concept, i.e. considering the wall is acting as a diagonal strut connecting the two loaded corners. The axial stiffness of the strut, K, is given by

$$K = \frac{E_\theta \times A}{L} \qquad [1]$$

where, E_θ, A and L are Young's Modulus, area and length of the strut, respectively.

The strength can be investigated also by applying the diagonal strut theory, that is the strength of the strut, F_u, is given as a function of the ultimate compressive strength of the strut, $f_{m\text{-}\theta}$, by the following equation

$$F_u = f'_{m-\theta} \times A \qquad [2]$$

It is important to note that this model is applicable only if all possible failure modes were suppressed except for the *CC* mode. However, the *CC* mode capacity must be known before hand in order to design the FRP to suppress all other failure modes. On the other hand the *CC* mode capacity is dependant on the FRP type, because, as demonstrated in Phase 1 of the test program, the axial strength of retrofitted masonry depends on the FRP type.

The following sections describe an analytical model developed to evaluate the behaviour of CMISF failing in *CC* mode. These sections are followed by design requirements to prevent the *SS* failure mode.

Proposed simplified model

In the proposed simplified model, the steel frame members were modeled using elastic beam elements connected by non-linear rotational spring elements at the beam-column joints. Assuming an orthotropic material behaviour for the masonry wall in the two principle directions, parallel and perpendicular to the bed joints. The effective *strut* area of the wall which, generally ranges between 10% and 25% of the column height multiplied by the thickness of the wall, or the thickness of the face shells in case of face shell mortar bedding was given by

$$A = \frac{(1-\alpha_c)\,\alpha_c\, h\ t_m}{\cos\theta} \qquad [3]$$

where, α_c is the ratio of the column contact length to the clear column height h, θ is defined as $\tan^{-1}\theta = (h/l)$, and l is the beam span. The parameter α_c representing the ratio between the column-wall contact length and the column height is given by Equation 4.

$$\alpha_c h = \sqrt{\frac{2\ (M_{pj} + 0.2\ M_{pc})}{t_m f'_{m-0}}} \leq 0.4h \qquad [4]$$

where, M_{pj} is the minimum of the plastic moment capacity of the column, the beam or the connection, referred to as the plastic moment capacity of the joint. M_{pc} is the column plastic moment capacity, f_{m-0} is the compressive strength of the masonry wall parallel to the bed joint, and t_m is the thickness of the wall or the face shell thickness in case of face shell mortar bedding.

Due to the fact that the walls behave as if they were *diagonally loaded*, constitutive relations, of orthotropic plates and statistical correlation between different hollow concrete masonry walls properties are used to obtain the Young's modulus, E_θ, of the wall in the diagonal direction given by the following equation

$$E_\theta = \frac{\alpha\ f'_{m-90}}{1.25\cos^4\theta + 2\cos^2\theta\sin^2\theta + \sin^4\theta} \qquad [5]$$

It was also suggested by El-Dakhakhni et al. [4] that, not only Young's modulus will change, but also the ultimate strength of the masonry wall in the θ direction, $f_{m-\theta}$. To account for this direction variation, and to relate E_θ to $f_{m-\theta}$ using the same relation relating E_{90} to f_{m-90}, i.e.

$$f'_{m-\theta} = \frac{E_\theta}{\alpha} \text{ where, } \alpha = \frac{E_{90}}{f'_{m-90}} \qquad [6]$$

The proposed *CC* model was used to model the solid unretrofitted and retrofitted CMISF specimens. The load-deflection relation of the bare, the unretrofitted and the retrofitted specimens are shown in Fig. 8-a, 8-b and 8-c, respectively along with test results for comparison. The model closely approximate the stiffness of the CMISF up to failure and appears to overestimate the strength of the unretrofitted specimen by 10 %, and underestimate that of the retrofitted specimen by 7%.

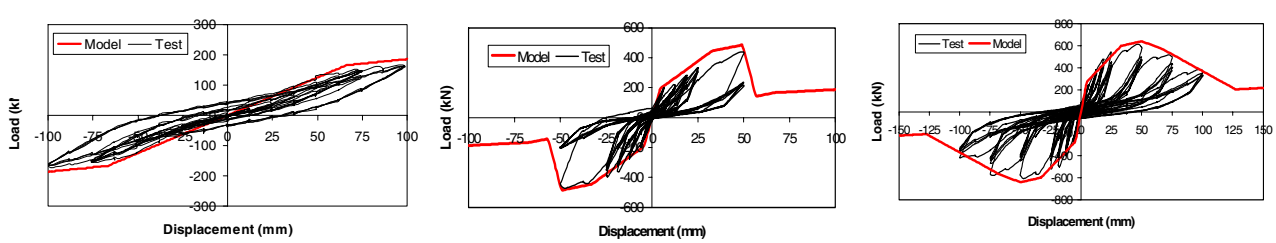

(a) (b) (c)

Fig. 8: Analytical model prediction of specimen responses

Eliminating the *SS* Mode

The *SS* mode is relatively complicated to model, this is due to the *uncertain* value of the friction coefficient between the masonry blocks (typically varying from 0.3 to 1.2 as suggested by Paulay and Priestley [5]) as well as the complex shear-compression interaction in the masonry wall (Hamid et al. [6]).

The elimination of the *SS* mode, which causes the *knee brace* effect on the frame (Paulay and Priestley [5]) is also of prime interest since it is a sudden, non-ductile mode of failure that causes severe damage to the frame columns at its mid height. It is also clear that due to the weak shear bond strength of the mortar bed joints, causing the *SS* mode, the full wall capacity presented in the *CC* mode could not be utilized.

The FRP shear strength, $f_{FRP\text{-}\tau}$, should be enough to prevent the *SS* mode of failure presented in the form of horizontal shear slip along a bed joint to take place. It is then required that the retrofitted bed joint can withstand this stress to safeguard against developing the *SS* mode of failure. Equations 8 (El-Dakhakhni [7]) gives the demand, $f_{\tau\text{-}d}$, of shear force per unit length at the retrofitted bed joints,

$$f_{GFRP-\tau} = \frac{1.5F_u \sin\theta}{h} - 0.3\,\frac{F_u \sin^2\theta}{h\cos\theta} = \frac{F_u \sin\theta}{h}\left(1.5 - 0.3\frac{\sin\theta}{\cos\theta}\right) \qquad [7]$$

In this previous equation the extra shear supply of shear resulting from the friction due to normal force resulting from the wall's own weight above the sliding bed joint, as well as any imposed gravity loads from the top beam as it deflects is neglected due to the uncertainty of which bed joint is weaker or where the slippage should occur, although it is suggested to be approximately in the mid height of the wall (Pauly and Priestley [5]) and the shrinkage of the wall itself that might result in a loss of contact between the top beam and the infill. In any case omitting these factors are on the safe side since their inclusion will result in a lesser FRP ratio to carry lesser shear, and also because of the small ratio of the walls' weight compared to the vertical component of the strut.

CONCLUSIONS

1. By eliminating the shear failure using properly selected FRP laminates, the long known anisotropy of masonry resulting from the complex shear-compression interaction along the weak mortar joints can now be eliminated. In this *engineered masonry-FRP composite wall*, the FRP laminate can supply the required shear strength, and the face shells will be provide the compression strength. The FRP laminates will also improve the compression strength of the face shells by means of stabilizing the out-of-plane buckling of the face shells and confining the face shells against in-plane tensile failure, thus allowing it to carry more loads.
2. Similar to the retrofitted assemblages, the FRP laminated maintain the full-scale wall structural integrity and prevented collapse and debris fallout, contain and localize the damage of the unreinforced masonry (URM) walls even after ultimate failure. No signs of distress were evident throughout the wall except at the vicinity of the corners. This keeps the face shells of all the blocks as one plate, thus reducing the possibility of the external walls or partitions spalling, which, in itself, a major source of hazard during earthquakes even if the whole structure remains safe and functioning. The masonry-FRP composite walls do not fail catastrophically as their URM counterparts. The FRP laminates resulted in a gradual prolonged failure, a stronger wall, more energy dissipation and apparent post peak strength. This will result in a larger response modification factor than that typically selected for the analysis of URM wall structures.

3. The FRP retrofitting technique enhances the infilled frame stiffness, strength, and post-peak behaviour.
4. The technique eliminates undesirable failure modes along with the uncertainties associated with their evaluation. The technique also facilitates modeling of the wall by minimizing the anisotropic behaviour of masonry due to the weak shear strength of the mortar joints.
5. The diagonal strut model will be adequate to model the retrofitted system since it will fail in corner crushing only with no shear failure or diagonal cracking. The retrofitting effect is accounted for by incorporating design parameter to account for the stiffness, strength, and ductility increase.
6. The proposed analytical technique predicts the lateral stiffness up to failure, and the ultimate load capacity of solid CMISF to an acceptable degree of accuracy. The technique accounts for the nonlinear behaviour that occurs in both the steel frame (due to formation of plastic hinges) and in the masonry wall (due to corner crushing).
7. The technique presents a macro-model that is more easy and practical to apply and require much less time than techniques based on treating the wall as a plate or discretizing the wall as a series of plane stress elements interconnected by a series of springs or contact elements.

ACKNOWLEDGEMENT

The work presented herein is a part of a study performed at Drexel University under Grant No. CMS-9730646 from the National Science Foundation (NSF). The results, opinions, and conclusions expressed in this paper are solely those of the authors and do not necessarily reflect those of the NSF. The authors would like to gratefully acknowledge the assistance of Edward Fyfe, Sarah Cruickshank, Robert Fyfe and Tylor Mass of Fyfe Co. LLC, California, for supplying and installing the GFRP. The authors would also like to thank Ms. Lucy El-Sherif and Dr. Tamer El-Raghy for their valuable suggestions.

REFERENCES

1. American Institute of Steel Construction (AISC), Inc. (1998), "Load & Resistance Factor Design-Structural Members, Specifications & Codes," Manual of Steel Construction, second edition, AISC.
2. Porter, M. L., and Tremel, P.M. (1987) "*Sequential Phased Displacement Procedure for TCCMAR Testing*" Third meeting of the joint Technical Coordinating Committee on Masonry Research, US-Japan Coordinated Earthquake Research Program, Sapporo, Japan.
3. El-Dakhakhni, W. W. and Drysdale, R. G., (2004) "3-D Finite Element Modelling of Masonry-Infilled Frames with Opening" Proc. 13th International Brick/Block Masonry Conference, Amsterdam, The Netherlands.
4. El-Dakhakhni, W. W., Elgaaly, M. and Hamid, A. A., (2003) "*Three-Strut Model for Concrete Masonry-Infilled Steel Fram*es" ASCE Journal of Structural Engineering, Vol. 129, No. 2, pp. 177–185.
5. Paulay, T. and Priestley, M. J. N. (1992) "Seismic Design of Reinforced *Concrete and Masonry Buildings*," John Wiley & Sons, Inc., New York, NY, USA.
6. Hamid, A. A., Ziab, G., and El Nawawy, O., (1987) "*Modulus of Elasticity of Concrete Masonry*" Fourth North American Masonry Conference. University of California at Los Angeles, Paper 7.
7. El-Dakhakhni, W. W. (2002) "*Experimental and Analytical Seismic Evaluation of Concrete Masonry-Infilled Steel Frames Retrofitted using GFRP Laminates*" Ph.D. thesis, Civil and Architectural Engineering Department, Drexel University, Philadelphia, PA, 19104, USA.